



*Original Article*

## Performance study of solar air heater duct having absorber plate with V down perforated baffles

Sunil Chamoli<sup>1\*</sup> and Narendra Thakur<sup>2</sup>

<sup>1</sup> Dehradun Institute of Technology University, Dehradun, Uttarakhand, 248001 India.

<sup>2</sup> Centre for Energy and Environment, National Institute of Technology, Hamirpur, 177005 India.

Received 12 February 2013; Accepted 5 December 2013

---

### Abstract

This paper presents results of a study of the performance of solar air heaters with V down perforated baffles as roughness on the air flow side of the absorber plate. Investigations have been carried out using a mathematical model to study the effects of ambient conditions, operating and design parameters on effective efficiency of such air heaters. The thermal and effective efficiencies differ only marginally at lower flow rates. With an increase in the flow rate, the difference between the thermal and effective efficiencies increases because of the increase in the pumping power. The results of the study are presented in the form of plots to show the effect of ambient, design and operating conditions on thermal and effective efficiency.

**Keywords:** thermal efficiency, effective efficiency, solar air heater, perforated baffles, insolation

---

### 1. Introduction

Flat-plate solar collectors are being used for thermal conversion to raise the temperature of fluid flowing through the collector. Conversion of solar radiations to thermal energy is mainly due to heat transfer coefficient between absorber plate and the fluid flowing in the collector. Several designs of solar air heaters have been developed over the years in order to improve their performance. A solar air heater is a simple device which heats air by utilizing solar energy and has many applications such as space heating, drying for industrial and agricultural purposes (Gupta and Kaushik, 2008). The thermal efficiency of solar air heater is less due to low heat transfer capability between absorber plate and fluid flowing in the duct. In order to make solar air heaters more efficient, thermal efficiency needs to be improved by the enhancing heat transfer rate. Vortex generators such as ribs, baffles, and winglets found feasible to enhance system performance.

Disturbance promoters increase fluid mixing and interrupt the development of thermal boundary layer, leading to the enhancement of the heat transfer. Chamoli *et al.* (2012) gave a detailed review of a large number of turbulence promoters investigated for solar thermal systems. The heat transfer enhancement occurred with solid baffles accompanied with a large increase in the friction factor is a serious concern. To overcome this adverse effect perforated baffles are used, as the perforated elements allow a part of the flow to pass through the holes, thus the hot zone and form drag are reduced. A number of heat transfer studies employed in a rectangular channel with perforated ribs attached were carried out on single or both the broad walls (Sara *et al.*, 2001; Liou *et al.*, 2002; Dutta *et al.*, 2005; Karwa *et al.*, 2005; Karwa and Maheswari, 2009; Ary *et al.*, 2012). The perforated elements allow a part of fluid to pass through holes causes a jet impingement of the fluid flow directly on heated surface that enhanced the heat transfer and a considerable reduction in pressure drop was observed. Increase in Reynolds number enhanced the heat transfer accompanied with an increase in pumping power requirement. It is thus necessary to take into account both the rate of collection energy and the pumping

---

\* Corresponding author.

Email address: mech.chamoli@gmail.com

power requirement i.e. thermohydraulic performance evaluation is required to optimize the geometrical parameters.

**2. Experimental Setup Detail**

An experimental test facility was designed and fabricated to study the effect of geometrical and flow parameters ratio in V down baffle geometry on the heat transfer and fluid flow characteristics of a rectangular duct. A schematic diagram of the experimental test rig is shown in Figure 1. The overall length of the solar air heater duct is 2,400 mm with a test section of 1,300 mm. The cross section of the test section is 350 (width) x 35 mm (depth) The entry and exit lengths are considered on the basis of ASHRAE standards (1977) which suggest minimum entry and exit lengths of  $5\sqrt{WH}$  and  $2.5\sqrt{WH}$  respectively for turbulent flow regime. The entire duct is insulated with 50 mm wool on top and 50 mm wooden blocks from other sides of the duct to ensure minimum heat loss to the environment. The test section consist of roughened test plate of thickness 3 mm painted black from the rear side and an electric heater is placed above the absorber plate to provide a constant heat flux of 1,000 W/m<sup>2</sup> made of series and parallel loops of Nichrome wire.

**3. Thermal and Thermohydraulic Performance of Solar Air Heater**

Rate of useful heat gain by air flowing through duct of solar air heater can be evaluated in terms of mean plate temperature by using the following equation

$$Q_u = A_p [I(\tau\alpha) - U_L(T_p - T_a)] \tag{1}$$

Rate of useful energy gain by air owing through duct of solar air heater can also be evaluated by using the following Hottel–Whillier–Bliss equation

$$Q_u = A_p F_R [I(\tau\alpha) - U_L(T_i - T_a)] \tag{2}$$

Thermal efficiency and heat removal factor can be written as

$$\eta_{th} = \frac{Q_u}{I A_p} = F_R \left[ (\tau\alpha) - U_L \left( \frac{T_i - T_a}{I} \right) \right] \tag{3}$$

$$F_R = \frac{\dot{m} C_p}{U_L A_p} \left[ 1 - \exp \left( - \frac{U_L A_p F'}{\dot{m} C_p} \right) \right] \tag{4}$$

Thermal efficiency can be written in terms of outlet fluid temperature as

$$\eta_{th} = F_o \left[ (\tau\alpha) - U_L \left( \frac{T_o - T_i}{I} \right) \right] \tag{5}$$

$F_o$  can be evaluated using the following equation

$$F_o = \frac{\dot{m} C_p}{U_L A_p} \left[ \exp \left( \frac{U_L A_p F'}{\dot{m} C_p} \right) - 1 \right] \tag{6}$$

Useful energy gain is evaluated using the equation

$$Q_u = \dot{m} C_p (T_o - T_i) \tag{7}$$

Based on Equation 7, thermal efficiency can be calculated as

$$\eta_{th} = \frac{\dot{m} C_p (T_o - T_i)}{I A_p} \tag{8}$$

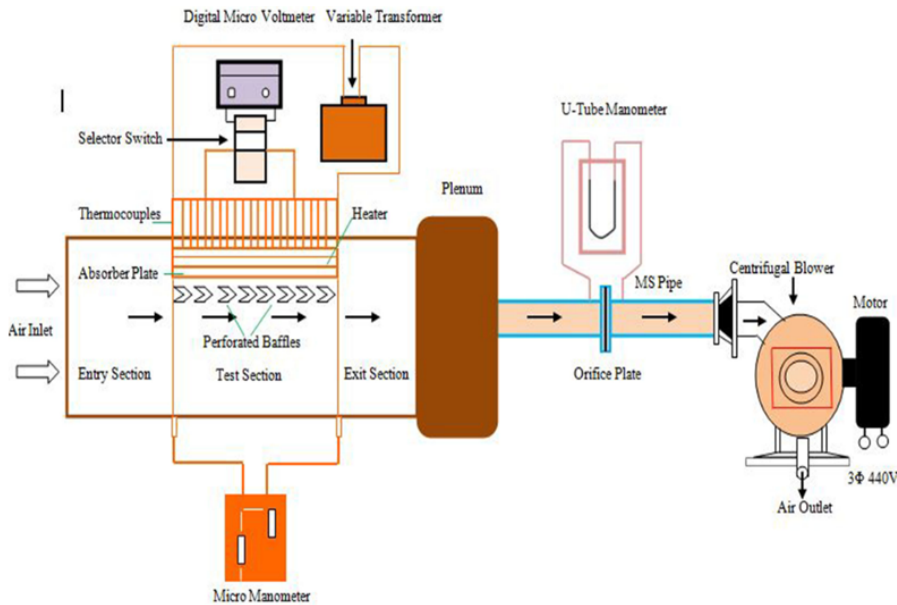


Figure 1. Schematic diagram of test setup.

Thermohydraulic performance of solar air heater is evaluated on the basis of effective efficiency and is written as

$$\eta_{eff} = \frac{Q_u - \frac{P_m}{C}}{IA_p} \quad (9)$$

where  $P_m$  the mechanical energy consumption for propelling is air through the duct and can be computed by the equation

$$P_m = \frac{\dot{m} \Delta P}{\rho} \quad (10)$$

Factor  $C$  is the conversion factor to convert mechanical energy to thermal energy and can be written as

$$C = \eta_{Th} \eta_{tr} \eta_m \eta_f \quad (11)$$

Pressure drop across the duct can be evaluated using the following relationship

$$\Delta P = \frac{4fLV^2\rho}{2D} \quad (12)$$

### 3.1 Mathematical model for performance prediction

A schematic diagram of the V-shaped perforated baffles is shown in Figure 2. To compute the thermal and thermohydraulic performance of V down perforated baffled roughened solar air heater the range of system and operating parameters considered for the study is given in Table 1 In order to evaluate the thermal efficiency from Equation 5 the value of  $U_L$  and  $F_o$  can be evaluated as following:

Overall heat loss coefficient is the sum of top, bottom and edge loss coefficients and written as

$$U_L = U_t + U_b + U_e \quad (13)$$

The  $U_b$  bottom heat loss coefficient is given below

$$U_b = \frac{k_i}{t_i} \quad (14)$$

The edge heat loss coefficient is given below

$$U_e = \frac{(W + L) \times L_1 \times k_i}{W \times L \times t_e} \quad (15)$$

Using the assumed value of the plate temperature, the value of top loss coefficient,  $U_t$  is computed by using the equation proposed by (Kline, 1975)

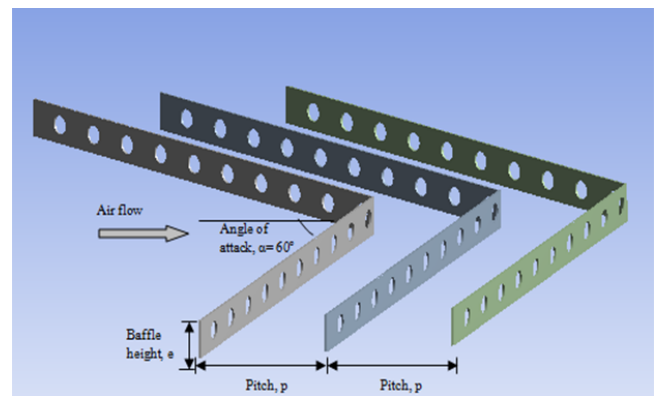


Figure 2. Schematic diagram of the V down perforated baffles.

Table 1. System and operating parameters.

		Parameter	Value/range
System parameters	Variable	Collector length (L), m	1-2
		Collector width (W), m	0.1-0.7
		Number of glass covers (N)	1-3
	Fixed	Collector height (H), m	0.035
		Transmittance-absorptance ( $\tau\alpha$ )	0.8
		Emittance of glass ( $\epsilon_g$ )	0.88
		Emittance of plate ( $\epsilon_p$ )	0.9
		Thickness of glass cover ( $t_g$ ), m	0.004
		Thickness of insulation ( $t_i$ ), m	0.05
		Thermal conductivity of insulation ( $K_i$ ), W/m-K	0.037
		Angle of attack ( $\alpha$ ), deg	60°
		Relative roughness pitch (P/e)	2
		Relative roughness height (e/H)	0.4
Open area ratio ( $\beta$ )	12%		
Operating parameters	Fixed	Ambient temperature ( $T_a$ ), K	300 K
	Variable	Temperature rise parameter ( $\Delta T/I$ ), m <sup>2</sup> K/W	0.002-0.025
		Wind velocity ( $V_w$ ), m/s	1-10
		Insulation (I), W/m <sup>2</sup>	500-1000

$$U_t = \left[ \frac{N}{\frac{c_t (T_p - T_a)}{T_p (N + f_t)} + \frac{1}{h_w}} \right]^{-1} + \left[ \frac{\sigma (T_p^2 + T_a^2) (T_p + T_a)}{1 + \frac{2 \times N + f_t - 1}{(\epsilon_p + 0.05 \times N (1 - \epsilon_p)) \epsilon_g}} \right]^{-1} \quad (16)$$

Where

$$h_w = 5.7 + 3.8 \times V_w$$

$$c_t = 365.9 \left[ 1 - 0.00883 \times S + 0.0001298 \times S^2 \right]$$

$$f_t = \left( 1 - 0.04 \times h_w + 0.0005 \times h_w^2 \right) (1 + 0.091 \times N)$$

To compute top loss coefficient, an initial approximation of mean plate temperature is considered as

$$T_p = \frac{T_o + T_i}{2} + 10^\circ C \quad (17)$$

Where

$$T_o = T_i + \Delta T \quad (18)$$

Rise in temperature of air is calculated as

$$\Delta T = \frac{\Delta T}{I} \times I \quad (Q_{u1}) \quad (19)$$

Useful energy gain ( $Q_{u1}$ ) is calculated by using Equation 1 as

$$Q_{u1} = A_p \left[ I(\tau\alpha) - U_L (T_p - T_a) \right] \quad (20)$$

To verify the value of useful energy gain calculated in Equation 20; it is computed using the following equation as

$$Q_{u2} = A_p F_o \left[ I(\tau\alpha) - U_L (T_o - T_i) \right] \quad (21)$$

The collector efficiency factor ( $F_p$ ) and heat removal factor ( $F_o$ ) are determined as

$$F_p = \frac{h}{h + U_L} \quad (22)$$

$$F_o = \frac{\dot{m} \times C_p}{A_p \times U_L} \left[ 1 - \exp \left( - \frac{A_p U_L F_p}{\dot{m} C_p} \right) \right] \quad (23)$$

Where convective heat transfer coefficient

$$h = \frac{Nu \times K}{D} \quad (24)$$

The Nusselt number is calculated using the correlation developed from experimental results, which is reproduced below,

$$Nu = 0.0296 Re^{0.7848} \left( \frac{P}{e} \right)^{0.3007} \left( \frac{e}{H} \right)^{-0.6774} \left( \beta \right)^{-0.3571} \exp \left[ -0.2548 \ln \left( \frac{P}{e} \right)^2 \right] \exp \left[ -0.4406 \ln \left( \frac{e}{H} \right)^2 \right] \exp \left[ -0.0863 \ln (\beta)^2 \right] \quad (25)$$

If difference between  $Q_{u1}$  and  $Q_{u2}$  is found to be more than 0.1% of  $Q_{u1}$  than new value of mean plate temperature was computed using the following correlation as

$$T_p = T_a + \frac{I(\tau\alpha) - \frac{Q_{u2}}{A_p}}{U_L} \quad (26)$$

Above steps repeated till the difference between  $Q_{u1}$  and  $Q_{u2}$  is in the desired range. The friction factor is calculated using the correlation developed from experimental results, which is reproduced below,

$$f = 0.632 Re^{-0.18} \left( \frac{P}{e} \right)^{-0.16} \left( \frac{e}{H} \right)^{1.05} (\beta)^{-0.13} \quad (27)$$

The thermal efficiency is calculated from useful heat gain  $Q_{u1}$ , the average of  $Q_{u1}$  and  $Q_{u2}$  and defined as

$$\eta_{th} = \frac{Q_u}{I \times A_p} \quad (28)$$

The effective efficiency is calculated from Equation 9. The calculations are repeated for the next set system and operating parameters given in Table 1. To perform all the calculations a code in Matlab is generated.

#### 4. Results and Discussion

Figure 3 shows the variation of thermal efficiency of roughened and smooth duct solar air heaters as a function of flow rates and it is observed with increase in flow rates the thermal efficiency starts increasing and after a certain flow rate it is saturated this is due to the reason that on increasing flow rate the rate of heat transfer increases and after certain value of flow rate the temperature difference in the fluid is nearly same thus no more heat transfer is possible on increasing flow rate and thermal efficiency starts saturating. It is also observed from Figure 3 that for the entire range of flow rates

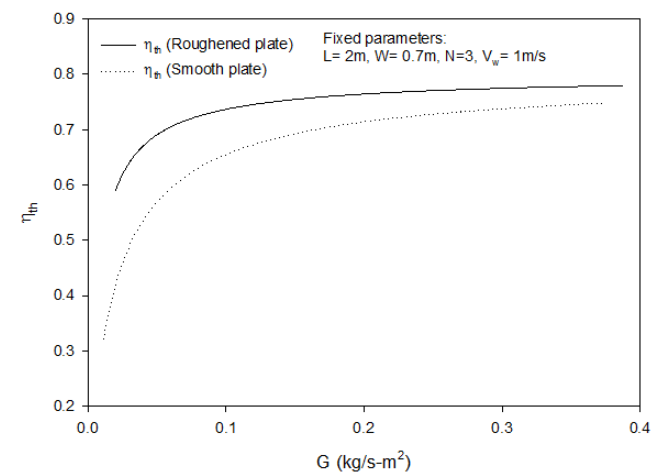


Figure 3. Thermal efficiency comparison of roughened and smooth duct solar air heater for fixed value of insolation ( $I=1,000$   $W/m^2$ ).

the thermal efficiency of roughened solar air heater is higher than smooth duct solar air heater. The thermal efficiency of roughened solar air heater decreases with an increase in wind velocity from 1 m/s to 10 m/s shown in Figure 4. With an increase in the wind velocity the heat transfer coefficient of wind increased which reduces the useful heat gain and thus the thermal efficiency is low. The variation of thermal efficiency as a function of the temperature rise parameter for different values of insolation is shown in Figure 5 and it is observed that thermal efficiency decreases with an increase in the temperature rise parameter and obtained maximum value for insolation of 1,000 W/m<sup>2</sup>. With the decrease in the insolation the useful heat gain decreases and thus the lower value of thermal efficiency is obtained. Figure 6 shows the variation of thermal and effective efficiency as a function of temperature rise parameter for a fixed value of insolation and it is observed that for higher values of temperature rise parameter the thermal efficiency overcome the effective efficiency due to increase in pumping power requirement for high flow rates.

The variation of effective efficiency of roughened solar air heater as a function of temperature rise parameter for different values of wind velocity is shown in Figure 7. It is observed that the effective efficiency starts to increase with an increase in the temperature rise parameter and attained a maximum value and then starts to decrease. This is due to fact that with an increase in the temperature rise parameter the corresponding pumping power requirement to propel air also increased, thus after a certain value of temperature rise parameter the pumping power overcome the useful heat gain and the effective efficiency starts to decrease. It is also observed that the effective efficiency attained maximum value for wind velocity of 1 m/s and for the lowest of 10 m/s. With increasing wind velocity the convective heat transfer coefficient of air increases which reduces the useful heat gain by increasing the top losses and thus the value of effective efficiency is less.

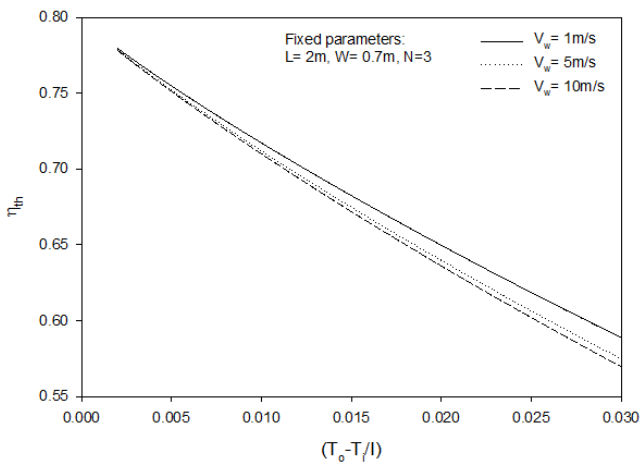


Figure 4. Variation of thermal efficiency of roughened solar air heater with wind velocity for fixed value of insolation ( $I = 1,000\text{ W/m}^2$ ).

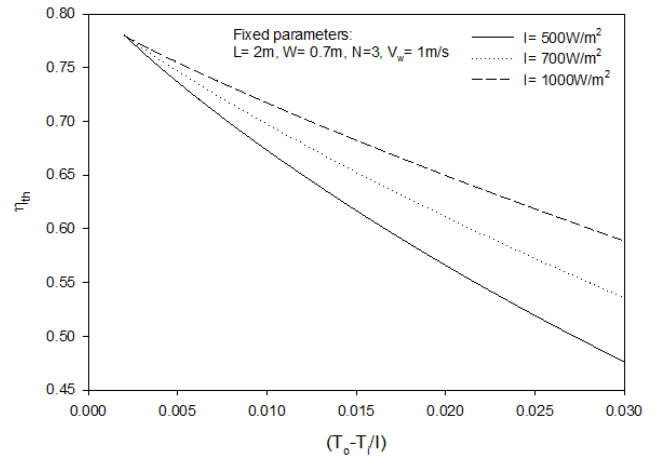


Figure 5. Variation of thermal efficiency of roughened solar air heater with different values of insolation.

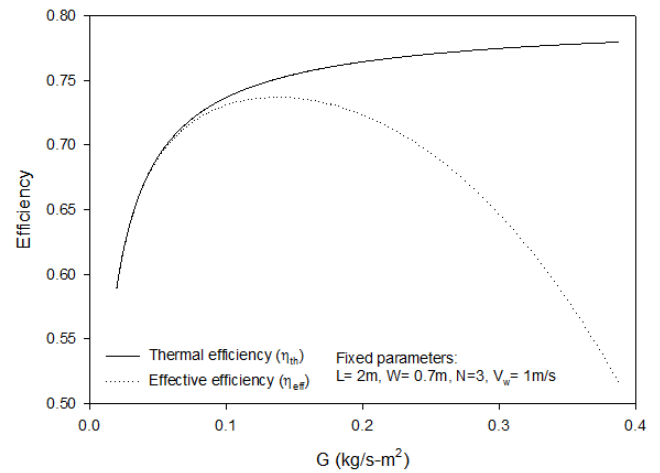


Figure 6. Variation of thermal and effective efficiency with flow rate for fixed value of insolation ( $I = 1,000\text{ W/m}^2$ ).

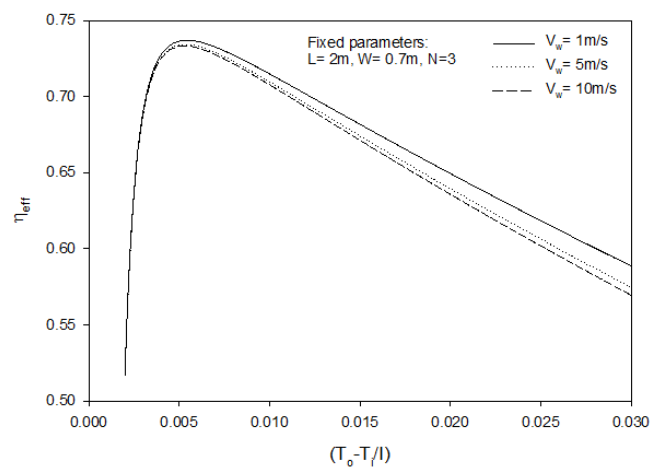


Figure 7. Variation of effective efficiency of roughened solar air heater with wind velocity for fixed value of insolation ( $I = 1,000\text{ W/m}^2$ ).

Figure 8 shows the variation of effective efficiency as a function of temperature rise parameter for different values of duct width. It is observed that effective efficiency is a strong function of duct width and it is observed that with increasing the duct width from 0.1 to 0.7 the effective efficiency increases as with an increase in the duct width the pumping power at the same flow rate is less for 0.7 than 0.1, which correspondingly gave higher effective efficiency at duct width of 0.7. The effect of duct length on the effective efficiency is shown in Figure 9. It is observed from Figure 9 that the effective efficiency increases with an increase in temperature rise parameter and attained a maximum value and then starts to decrease. It is also observed from Figure 9 that the effective efficiency is a strong function of duct length and with increase in duct length the effective efficiency increases as for a constant duct height the parameter (L/H) increases with an increase in the duct length and consequently the effective efficiency increases for higher values of temperature rise parameter.

The effect of the number of glass covers on the effective efficiency is shown in Figure 10 and it is observed that on increasing the number of glass covers the effective efficiency increases. This is due to the fact that with an increase in the number of glass covers the top losses to the surroundings is reduced which increases the useful heat gain and thus increases the effective efficiency.

The variation of effective efficiency as a function of temperature rise parameter for different values of insolation is shown in Figure 11. It is observed from Figure 11 that with an increase in insolation the performance improves as the rate of collection increased, thus the effective efficiency increases with an increase in the intensity of insolation.

**5. Conclusions**

The performance of roughened duct solar air heater with V down perforated baffles on the air flow side of

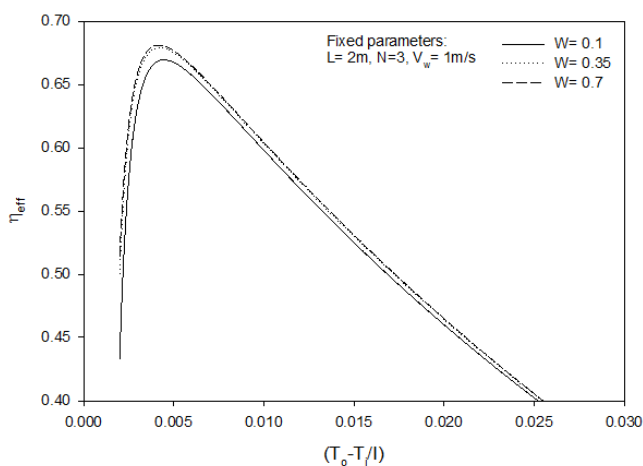


Figure 8. Variation of effective efficiency of roughened solar air heater with duct width for fixed value of insolation ( $I=1,000W/m^2$ ).

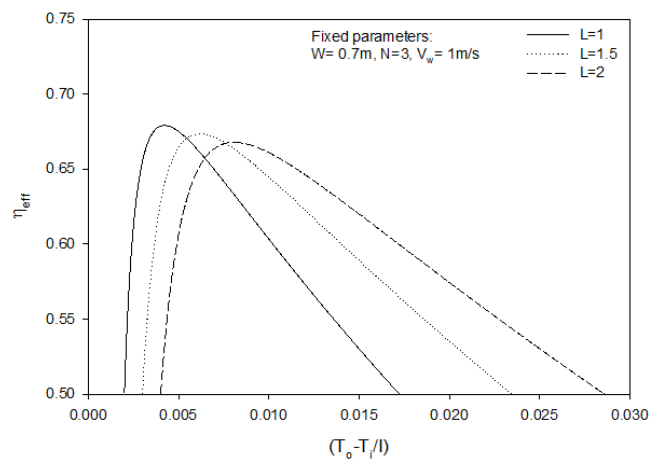


Figure 9. Variation of effective efficiency of roughened solar air heater with duct length for fixed value of insolation ( $I=1,000W/m^2$ ).

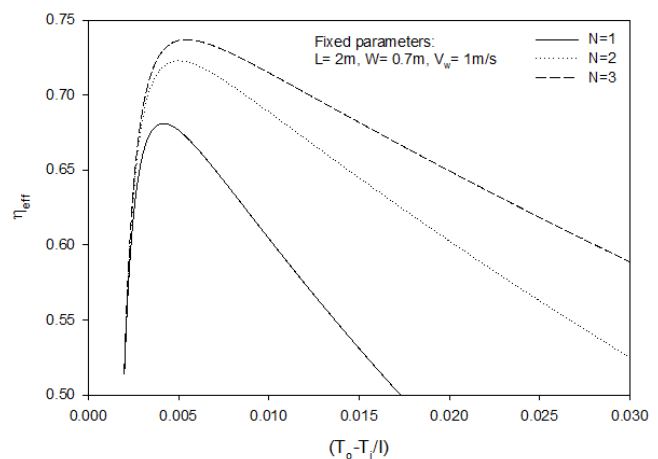


Figure 10. Variation of effective efficiency of roughened solar air heater with number of glass covers for fixed value of insolation ( $I=1000W/m^2$ ).

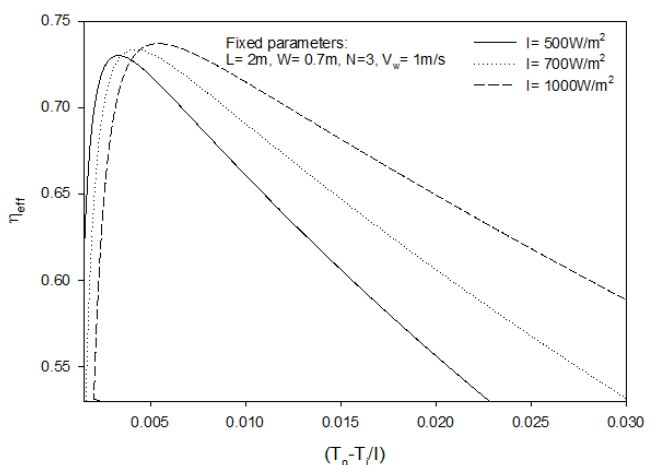


Figure 11. Variation of effective efficiency of roughened solar air heater with different values of insolation.

absorber plate has been studied using a mathematical model for a range of ambient, design and flow parameters ( $V_w = 1, 5, 10$  m/s,  $I = 500, 700, 1,000$  W/m<sup>2</sup>,  $L = 1, 1.5, 2$  m,  $W = 0.1, 0.35, 0.7$  m,  $N = 1, 2, 3$ ,  $G = 0.011 - 0.38$  kg/s-m<sup>2</sup>). The important findings of the study are:

1. With an increase in flow rates effective efficiency starts to increase and obtained a maxima and then starts to decrease; effective efficiency is highest for the flow rates from 0.75-1.5 kg/s-m<sup>2</sup>, thus it is desirable to operate the system within this range in order to obtain the maximum effectiveness from the system.

2. The thermal efficiency of the baffled duct solar air heater is about 20-80% higher than the smooth duct solar air heater. At low values of flow rates the enhancement is higher.

3. For higher values of flow rates the effective efficiency is significantly lower than thermal efficiency because of a significant increase in pumping power with an increase in the flow rate.

4. The results of the study are presented in the form of plots to show the effect of ambient, design and operating conditions on thermal and effective efficiency and it is observed that with an increase in insolation both the thermal and effective efficiency increases. The wind velocity has an impact on both thermal and effective efficiency and with an increase in wind velocity efficiencies decreases. Collector width and number of glass covers affects the effective efficiency and with an increase in both parameters the effective efficiency increases.

5. It is observed that both the geometrical and flow parameters of the present study have significant effects on the performance enhancement of V down perforated baffled roughened solar air heater duct.

## References

- American Society of Heating, Air Conditioning and Refrigeration Engineers. 1997. Method of testing to determine the thermal performance of solar collector. ASHRAE Standard, 93-97.
- Ary B.K.P., Lee M.S., Ahn S.W. and Lee D.H. 2012. The effect of the inclined perforated baffle on heat transfer and flow patterns in the channel. *International Communications in Heat and Mass Transfer*. 39, 1578-1583.
- Chamoli, S., Thakur, N.S. and Saini, J.S 2012. A review of turbulence promoters used in solar thermal systems. *Renewable and Sustainable Energy Reviews*. 16, 3154-3175.
- Dutta, P. and Hossain, A. 2005. Internal cooling augmentation in rectangular channel using two inclined baffles. *International Journal of Heat and Fluid Flow*. 26, 223-232.
- Gupta, M.K. and Kaushik, S.C. 2008. Exergetic performance evaluation and parametric studies of solar air heater. *Energy*. 33, 1691-1702.
- Karwa, R., Maheshwari, B.K. and Karwa, N. 2005. Experimental study of heat transfer enhancement in an asymmetrically heated rectangular duct with perforated baffles. *International Communications in Heat and Mass Transfer*. 32, 275-284.
- Karwa, R. and Maheshwari, B.K. 2009. Heat transfer and friction in an asymmetrically heated rectangular duct with half and fully perforated baffles at different pitches. *International Communications in Heat and Mass Transfer*. 36, 264-268.
- Kline, S.A. 1975. Calculation of flat plate collector loss coefficients. *Solar Energy*. 17, 79-80.
- Liou, T.M., Chen, S.H. and Shih, K.C. 2002. Numerical simulation of turbulent flow field and heat transfer in a two dimensional channel with periodic slit ribs. *International Journal of Heat and Mass Transfer*. 45, 4493-4505.
- Sara, O.N., Pekdemir, T., Yapici, S. and Yilmaz, M. 2001. Heat transfer enhancement in a channel flow with perforated rectangular blocks. *International Journal of Heat and Fluid Flow*. 22, 509-518.

## Nomenclature

$A_p$	surface area of absorber plate (m <sup>2</sup> )
$C$	conversion factor
$C_p$	specific heat of air (J/kg K)
$D$	hydraulic diameter of duct (m)
$e$	height of the baffle (m)
$e/H$	relative roughness height
$f$	friction factor
$F_o$	heat removal factor
$F_p$	collector efficiency factor
$G$	mass velocity of air (kg/s m <sup>2</sup> )
$H$	height of the duct (m)
$h$	heat transfer coefficient (W/m <sup>2</sup> K)
$h_w$	convective heat transfer coefficient of wind (W/m <sup>2</sup> K)
$I$	solar insolation (W/m <sup>2</sup> )
$K$	thermal conductivity of air (W/mK)
$K_i$	thermal conductivity of insulation (W/mK)
$L$	length of test section (m)
$L_1$	thickness of edge (m)
$\dot{m}$	mass flow rate of air (kg/s)
$N$	number of glass covers
$Nu$	Nusselt number
$P$	spacing between baffles (m)
$P/e$	relative roughness pitch
$P_m$	pumping power (W)
$\Delta P$	pressure drop across test section (Pa)
$Q_u$	useful heat gain (W)
$Re$	Reynolds number
$T_i$	temperature of fluid at inlet (K)
$T_o$	temperature of fluid at outlet (K)
$T_p$	mean temperature of absorber plate (K)

$T_f$	bulk mean temperature of flowing fluid (K)
$\Delta T$	air temperature rise across the duct ( $^{\circ}\text{C}$ )
$\Delta T/l$	temperature rise parameter ( $\text{m}^2 \text{K}/\text{W}$ )
$t_e$	thickness of edge insulation (m)
$U_L$	overall heat loss coefficient ( $\text{W}/\text{m}^2\text{K}$ )
$U_t$	top loss coefficient ( $\text{W}/\text{m}^2\text{K}$ )
$U_b$	bottom loss coefficient ( $\text{W}/\text{m}^2\text{K}$ )
$U_e$	edge loss coefficient ( $\text{W}/\text{m}^2\text{K}$ )
$W$	width of the duct (m)

**Greek**

$\alpha$	angle of attack of flow (degree)
$\beta$	open area ratio
$\rho_{\text{air}}$	density of air at bulk mean air temperature ( $\text{kg}/\text{m}^3$ )
$\mu$	dynamic viscosity of air at bulk mean temperature (Pa-s)
$\epsilon_p$	emittance of plate
$\epsilon_g$	emittance of glass cover
$\eta_{th}$	thermal efficiency
$\eta_{eff}$	effective efficiency
$\eta_t$	thermal power plant efficiency
$\eta_{Tr}$	transmission efficiency
$\eta_m$	motor efficiency
$\eta_f$	pump efficiency
$(\tau\alpha)$	transmittance absorbtance product of glass cover